Cotton Valley Production Stimulation Hydrofracture

Microseismic Monitoring & Imaging Phasell (CGU21-9 Fracture Imaging)

Union Pacific Resources Sponsored Industry Consortium

Data Collection & Analysis Report
Prepared by ARCO Exploration & Production Technology

July 1997

Robert J. Withers
Robert P. Dart

Table of Contents

1. Introduction

This report is a summary of the data acquisition and analysis of PhaseII fracture imaging at the Carthage Cotton Valley test site. PhaseII of this project consisted of recording data from both the CGU21-9 and CGU22-9 seismic monitoring arrays during the production fracturing of the CGU21-9 well which took place in three stages on July 14, 16, and 18. A 48 level hydrophone array was also placed in the nearby CGU22-7 well in an attempt to collect additional data for the fracture analysis. The CGU21-9 well was one of the two original monitor wells utilized in the recording of the CGU21-10 fracture stimulation. The seismic monitoring array in the annulus of this well was recorded during its fracture stimulation in an attempt to collect data in a single well imaging configuration.

2.0 Field Recording

2.1 Recording Configuration

With the exception of the addition of the hydrophone array in the CGU22-7 well the recording configuration for this phase of the experiment was the same in all respects as that of the original phase. A complete discussion of the original deployment aspect of this project may be found in the SPE paper (SPE38577) which was published by the Union Pacific Resources Company. A complete discussion of the recording hardware and software utilized in the seismic data acquisition may be found in the "Cotton Valley Production Stimulation Hydrofracture Microseismic Monitoring & Imaging" report presented to the UPRC sponsored consortium by ARCO.

It should be noted that Appendices 1 and 2 provide 2 different channel configurations for this experiment. On the 14th and 16th the hydrophone array was included in the recording configuration and is evidenced in Appendix 1. On the 18th the hydrophone array was removed from the recording configuration and is evidenced in Appendix 2. Additionally, because of some confusion in labeling of connectors the two connectors for the CGU22-9 array were plugged together incorrectly. This resulted in a reversal of the location of the channels from this array in the recorded data stream over that of the first phase of this experiment. Anyone performing any detailed analysis of this data should be aware of this and compare these configurations to that of the one contained in the report on the first phase of this experiment.

2.2 Hydrophone Array

The CGU22-7 production well was identified as a candidate for the use of a hydrophone array during this phase of the experiment. Figure 1 presents a plan view of the four wells involved in this phase. Figure 2 is a cross-sectional view

of the wells with the associated monitor arrays displayed. The hydrophone array consisted 48 individual hydrophone elements on a 50 foot vertical spacing. The array was constructed for ARCO by Tescorp Seismic Products and utilized the Benthos AHQ-1 hydrophone element. The cable had no internal support member as it was originally designed to be attached to production tubing during deployment. Although never utilized in this manner, it was used for one season of recording at ARCO's drill cuttings disposal site on the North Slope of Alaska. In that application the array was deployed inside production tubing and was clamped to common wireline cable with clamps designed specifically for that application to provide the needed support. This same system was utilized for deployment in the CGU22-7 well. The array was placed in the well with the top element at a depth of 5270 feet and the bottom element at a depth of 5975 feet.

A considerable amount of tube wave noise was recorded on the array in the Alaska application and not much of the data was useful in supporting the geophone array event solutions. It was hoped in this situation that the array would provide the needed support for the CGU22-9 monitor array as very little data was expected from the CGU21-9 monitor array. Unfortunately, there was very little activity recorded on the hydrophone array at all. In fact, there was so little activity evidenced on it that it was removed from the recording configuration for the final day of recording on 07/18. When it was attempted to remove the array from the well on 07/19 it was found to be stuck and no attempts to free it were successful. The wireline cable was cut and a workover rig was moved onto the location to extricate the cable from the well. This was a lengthy and costly effort which resulted in the destruction of the hydrophone array.

2.3 CGU21-9 Perforation Shots

The perforation shots executed in the CGU21-9 well on July 17 in preparation for the final stage of fracturing on the 18th were recorded on the seismic monitoring arrays. This data was needed to provide additional control and QC of geophone pod orientation for the CGU22-9 array to support event location in this single well solution situation.

3.0 Event location analysis

3.1 Geophone Pod Orientation

The rotoscan logs which were run after installation of each of the geophone arrays during the first phase of this project were analyzed by Branagan & Associates to produce a summary of the physical orientations of each of the geophone pods. With events only being detected on the CGU22-9 array it was necessary to use the results of this analysis in the Hodogram calculations performed in Fastrak in order to locate the origins of these events.

Figures 3 through 11 present the Hodogram analysis of three of the geophone pods from the CGU22-9 well. Figures 3, 6, and 9 are Hodogram plots from an application developed by Robert Withers. These plots are for pods 9, 14, and 24 respectively and were derived from primacord shots taken during the first phase of the project. For pod 9 the primacord shot at a depth of 7742 feet was selected and an angle of approximately 160 degrees is indicated. The shot at 8054 feet was used for Pod 14 indicates an angle of 140 degrees. Finally, the shot at 8754 feet was used for Pod 24 and it indicates an angle of approximately 115 degrees. Analyzing the geometry of the wells we find that the CGU21-10 well in which the primacord shots were taken is 20.9 degrees off of the north/south axis with respect to the CGU22-9 well which contains the array being analyzed. Taking this additional rotation into account we find rotation angles for each of these pods of 180, 160, and 135 degrees. Then allowing an additional rotation of 180 degrees for the polarity uncertainty we arrive at the following table:

Pod #	Hodogram Angle	Corrected Angle	Polarity Reversal	Rotoscan Angle
Pod 9	160	180	0	6
Pod 14	140	160	340	349
Pod 24	115	135	315	327

We find very good agreement between these two very different and independent methods of determining the physical orientation of the geophone pods. With this agreed upon the angles for all pods were taken from the Branagan summary and entered into the Fastrak database. With these angles now in place Figures 4, 7, and 10 were produced in Fastrak using primacord shots. In each case we find that the Hodogram points at the CGU21-10 well. Then Figures 5, 8, and 11 were produced in Fastrak using one of the perforation shots from the CGU21-9 well taken on 07/17/97 and we find the Hodogram to point to that well in all three cases. With this verification complete we could proceed with the location of the events detected during PhaseII using the Hodogram to point to the origin of each selected event.

4.0 Fracture interpretation

During the three days of recording a total of 1,836 events were detected and recorded to disk. The following table presents a breakdown of the distribution of these detected events over that period:

		Detected	Located
07/14/97	Stage 1	23	
	Stage 2	127	
	Stage 3	254	
	Stage 4	146	
	Total	**550**	**120**
07/16/97	Stage 1	23	
	Stage 2	17	
	Stage 3	47	
	Stage 4	224	
	Total	**311**	**21**
07/18/97	Stage 1	109	
	Stage 2	84	
	Stage 3a	281	
	Stage 3b	151	
	Stage 4a	269	
	Stage 4b	81	
	Total	**975**	**23**

Within Fastrak the process of locating an event involves the following steps. A pod which has both good P wave and S wave arrivals is chosen to begin the analysis. This pod does not necessarily have to be at the apex of the hyperbola at this point. Depth will be determined in the final step. With a pod selected, the shear wave arrival is picked and locked in place. Then we move up to the map window and grab the event and begin moving it about until the calculated P wave curve coincides with the P wave arrival for that pod. As we fine tune this pick the Hodogram will then point to the origin of the event. We then move the event to that location and move it in and out along the axis of the Hodogram until the calculated P wave curve once again coincides with the P wave arrival. Finally, the event is moved up and down in depth until the calculated P and S wave hyperbolas match the data and we are done and the solution is accepted.

The solutions thus produced for the 164 located events are summarized in Appendix 3. The data were analyzed as 3 separate injections and cross referenced with the injection bottom hole pressures and rates.

4.1 7/14/97 Fracture Results

As far as event quality goes this first day of recording was by far the best of all three days. The events were seen on a large number of the pods in the CGU22-9 monitor array. However, there were a large number of the detected events which contained only shear wave energy or a very small amount of P wave energy. In a single well solution events such as this are not locatable since we need the P wave energy to determine both the event origin and range from the monitor array. Because of this problem every detected event was displayed in Fastrak and given a ranking based on amplitude and presence of P wave energy. These summaries were then distilled down to only the two and three "*" events for possible location. These distilled summaries are presented in Appendix 4. Figure 12 shows a typical shear wave only event which can be compared with Figure 13 which shows a good high quality event. Figure 14 shows a more typical event with good shear wave energy and rather minimal P wave energy.

Figures 17 and 18 present FracView displays of the located events for this fracture. They show a very definite asymmetrical fracture trending to the northeast with very well contained height. It is possible that some of the events on the southwest wing of the fracture have intersected with the fracture propagated from the CGU21-10 well in Phase1 of this experiment. There is also a curve to the north evidenced at the tip of this fracture which may also indicate an intersection with the CGU21-10 fracture.

4.2 7/16/97 Fracture Results

This recording day yielded the least number of detected events of all three days of recording. These were all very low quality events as evidenced by a typical event for this day shown in Figure 15. Figures 19 and 20 show the FracView displays of the located events for this day. Although there is some indication of a trend in the expected direction of the fracture the limited and variable nature of the locations do not support any meaningful interpretation of this fracture. The quality of the data is such that the events located to the northwest cannot be relied upon as having originated there.

4.3 7/18/97 Fracture Results

Although this recording day yielded the highest number of detected events the majority of them were extremely low amplitude and quality. A typical event for

this day is seen in Figure 16. Figures 21 and 22 show the FracView displays of the located events for this day. These solutions can only be interpreted as random in nature with no definition of a fracture orientation. This day was also marked by an apparent loss of signal from a number of the deeper geophone pods in the CGU22-9 receiver array.

5.0 Summary

While the data quality for this second phase of the experiment was much lower than that of the first phase, a meaningful and valuable interpretation of the fracture created on the first day was nonetheless achieved. There is a definite asymmetrical orientation to this fracture trending more to the northeast. This trend matches that observed in the CGU21-10 fracture created during PhaseI of this experiment. Due to the geometry of the monitor arrays with respect to the treatment well in PhaseI of this experiment there were some questions as to whether or not it would be possible to detect events occurring on the far wing of the fracture if it existed. In this phase of the experiment, however, we have a situation where the monitor array is situated broadside to the expected plane of the fracture and we would expect to be able to detect events equally from both wings if they existed. In addition, we have added the Hodogram analysis in this phase to point to the origins of the events. So, while there are some events which were located near the CGU21-9 wellbore and to the southwest, there can be no doubt that the primary direction that this fracture took was to the northeast. There may also have been some intersection with the fracture produced in the CGU21-10 well.

This would indicate that in future experiments of this sort where there may be some question as to preferred fracture orientation serious consideration should be given to the positioning of the monitor arrays and possible use of three or more arrays.

As to the integrity of the monitor arrays at this experiment site the following conclusions must be made. First, since there was no activity evidenced on the CGU21-9 array either in the form of noise during the pumping operations or event energy it should be considered as dead and no longer useable. Secondly, the CGU22-9 array showed continued deterioration during this second phase of the experiment and its usefulness in any future experiments should be seriously questioned.

References

Walker, R. N. Jr., 1997; Cotton Valley Hydraulic Fracture Imaging Project, SPE 38577.

Withers, R. J., Dart, R. P., 1997; Cotton Valley Production Stimulation Hydrofracture Microseismic Monitoring & Imaging, Data Collection & Analysis Report.

Figures

Figure 1 Plan view of experiment site with CGU22-7 well added for hydrophone array which was not used in Phasel

Figure 2 Cross-section view of site showing deployed receivers. Note high location of hydrophone array

Figure 3 Hodogram analysis of Primacord shot for Pod 9 using Withers program

Figure 4 Hodogram analysis of Primacord shot for Pod 9 using Fastrak

Figure 5 Hodogram analysis of Perf shot for Pod 9 using Fastrak

Figure 6 Hodogram analysis of Primacord shot for Pod 14 using Withers program

Figure 7 Hodogram analysis of Primacord shot for Pod 14 using Fastrak

Figure 8 Hodogram analysis of Perf shot for Pod 14 using Fastrak

Figure 9 Hodogram analysis of Primacord shot for Pod 24 using Withers program

Figure 10 Hodogram analysis of Primacord shot for Pod 24 using Fastrak

Figure 11 Hodogram analysis of Perf shot for Pod 24 using Fastrak

Figure 12 Typical event with predominantly shear wave energy. Events such as this are unlocatable with only a single well solution because of the missing P wave information

Figure 13 Good high quality event easily located with a single well solution through the use of the Hodogram analysis of P wave first arrival to point to the event origin

Appendices

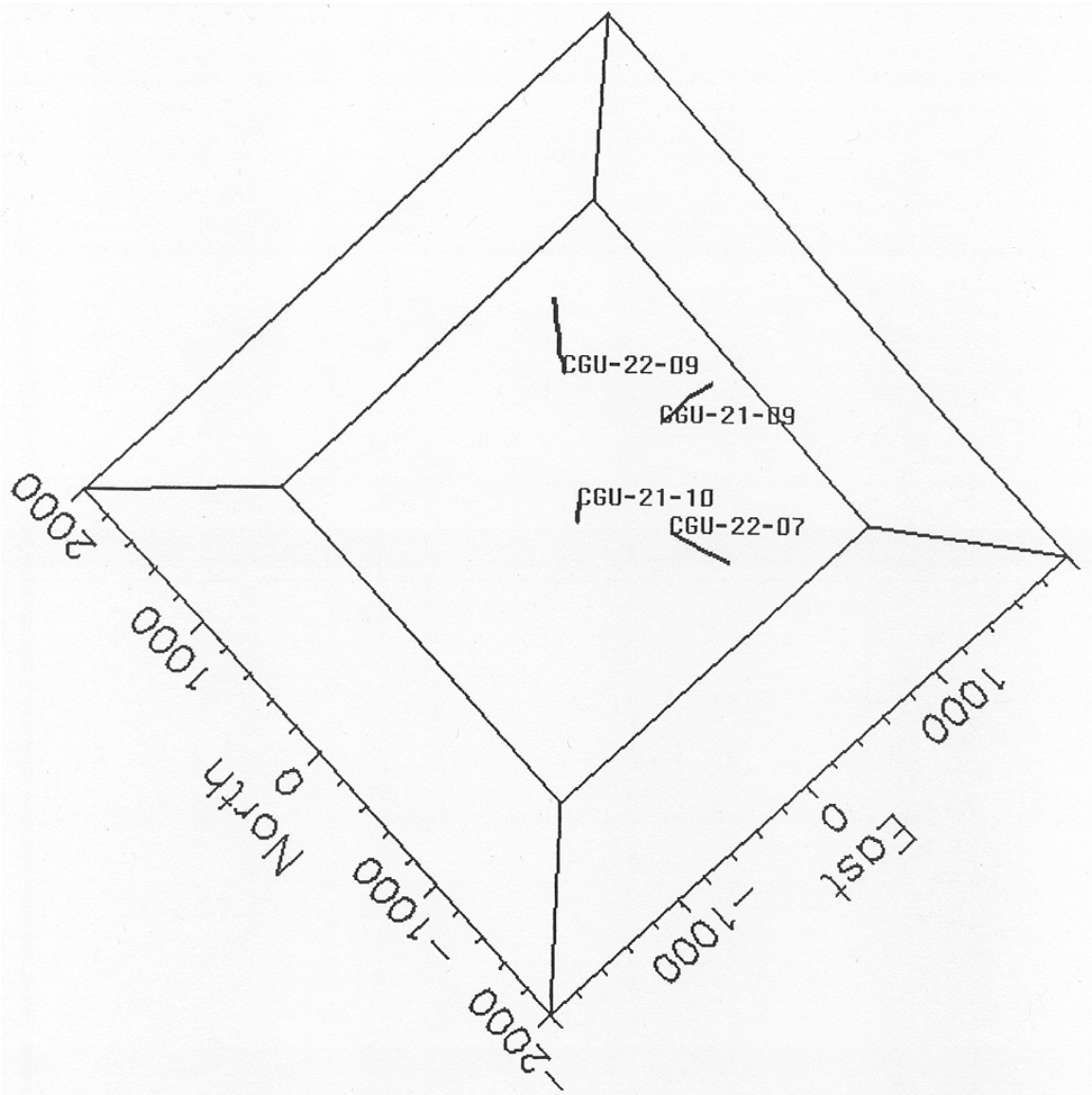

Cotton Valley Fracture Monitor - Phasell
Plan View of Well Geometry

Figure 1

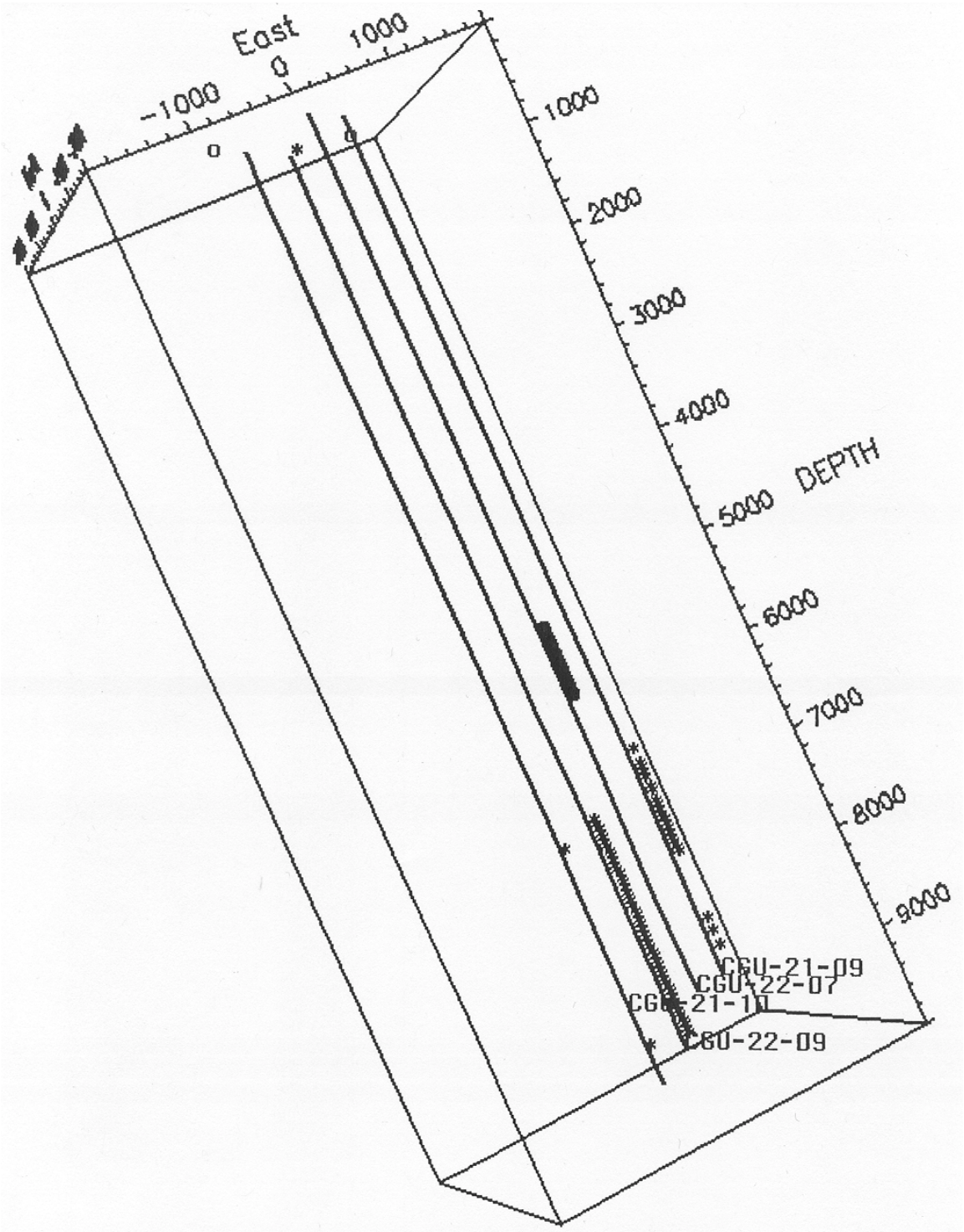

Cotton Valley Fracture Monitor - Phasell
Well & Receiver Diagram

Figure 2

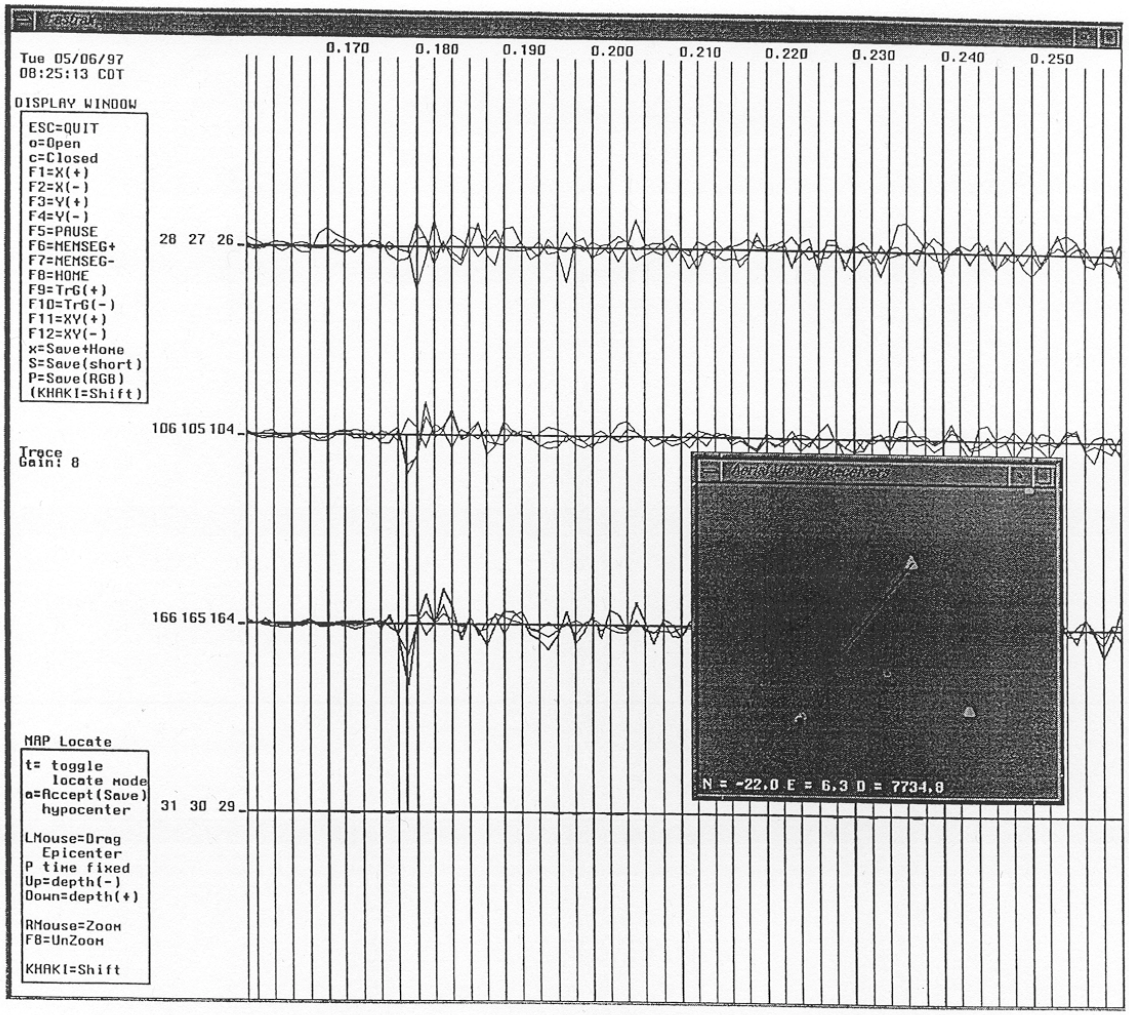

Primacord Hodogram Analysis - Pod 9

Figure 4

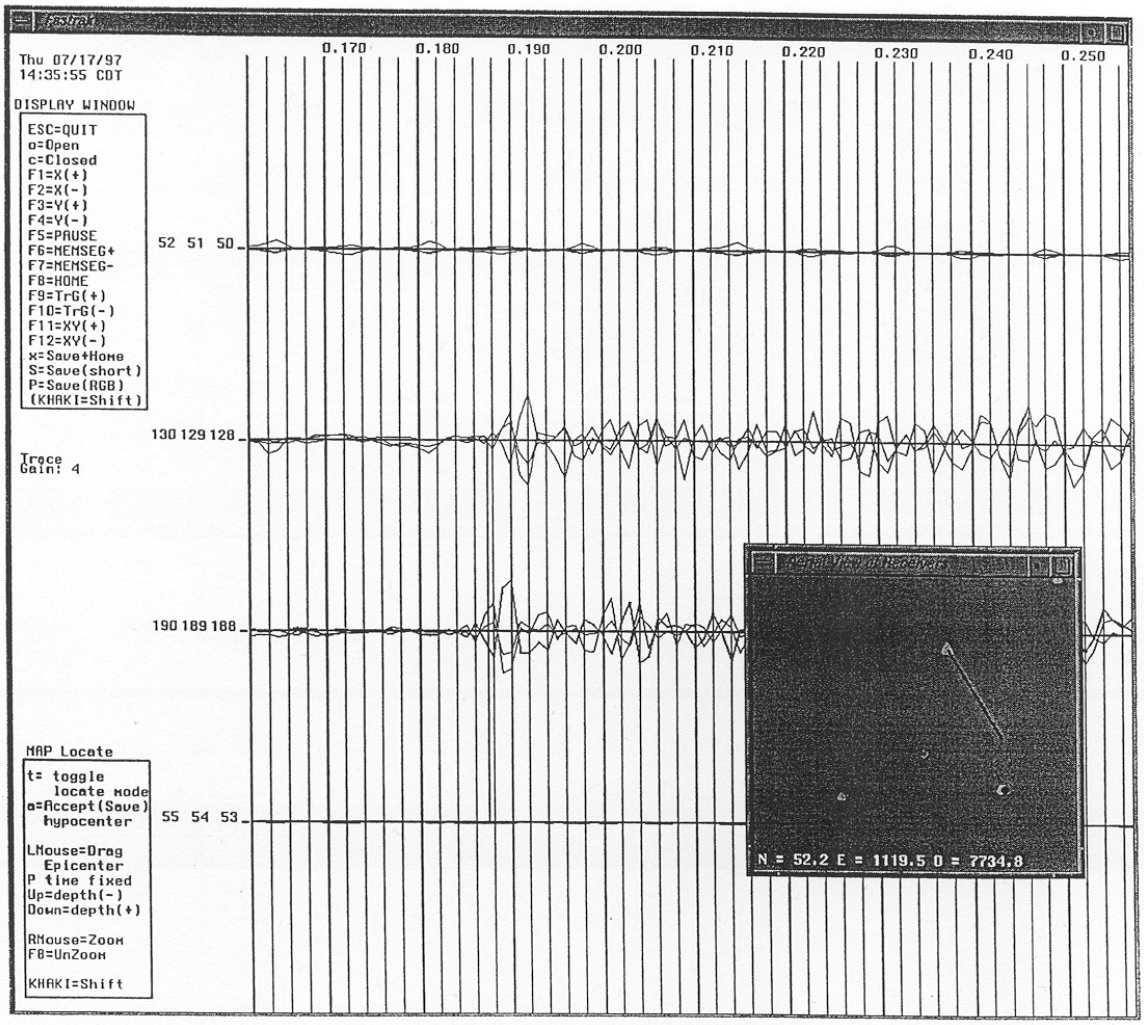

Perf Shot Hodogram Analysis - Pod 9

Figure 5

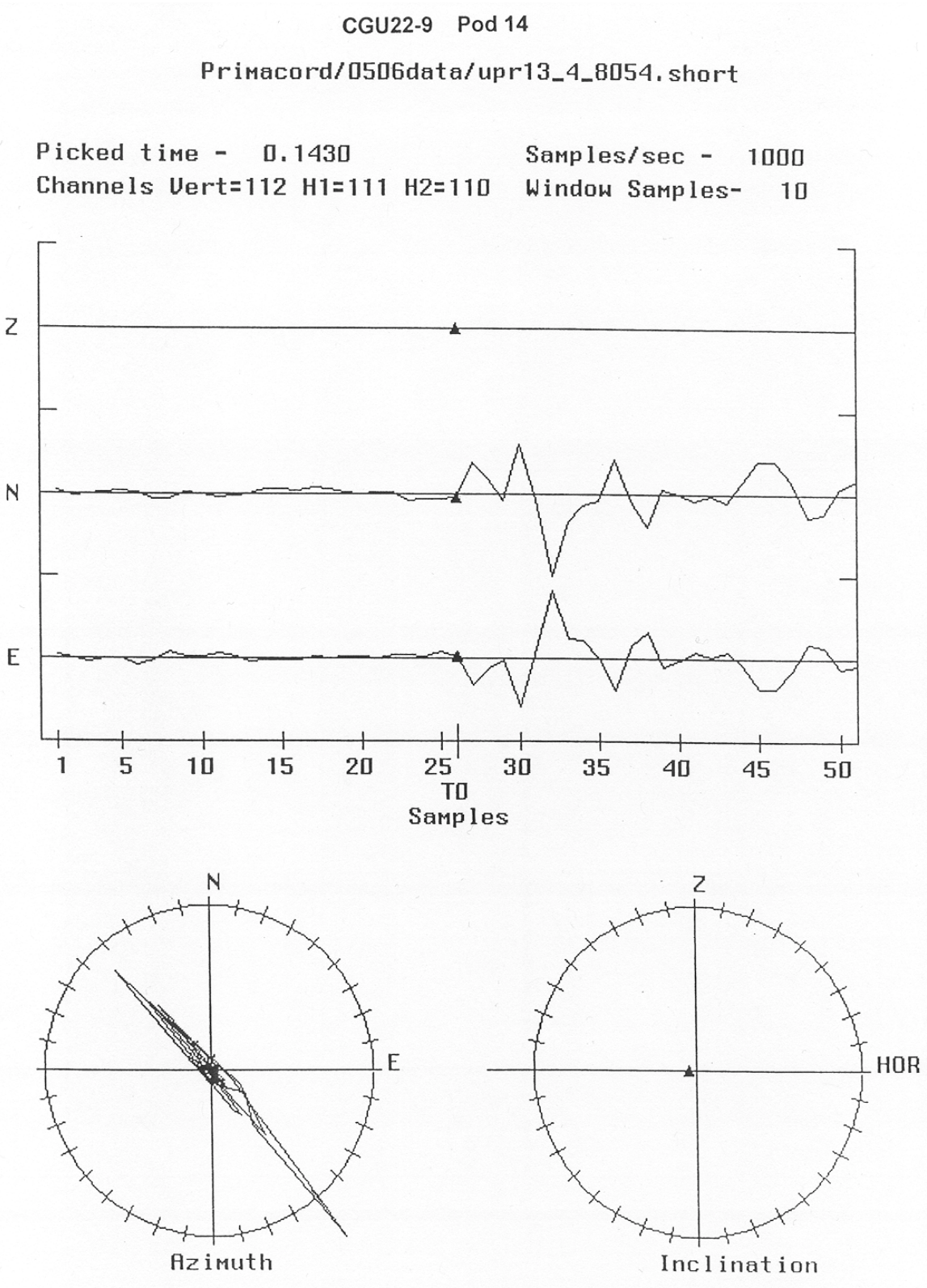
CGU22-9 Pod 14
Primacord/0506data/upr13_4_8054.short
Picked time - 0.1430
Samples/sec - 1000
Channels Vert=112 H1=111 H2=110
Window Samples- 10
Z
N
E
1
5
10
15
20
25
30
35
40
45
50
TO
Samples
N
E
Azimuth
Z
HOR
Inclination

Figure 6

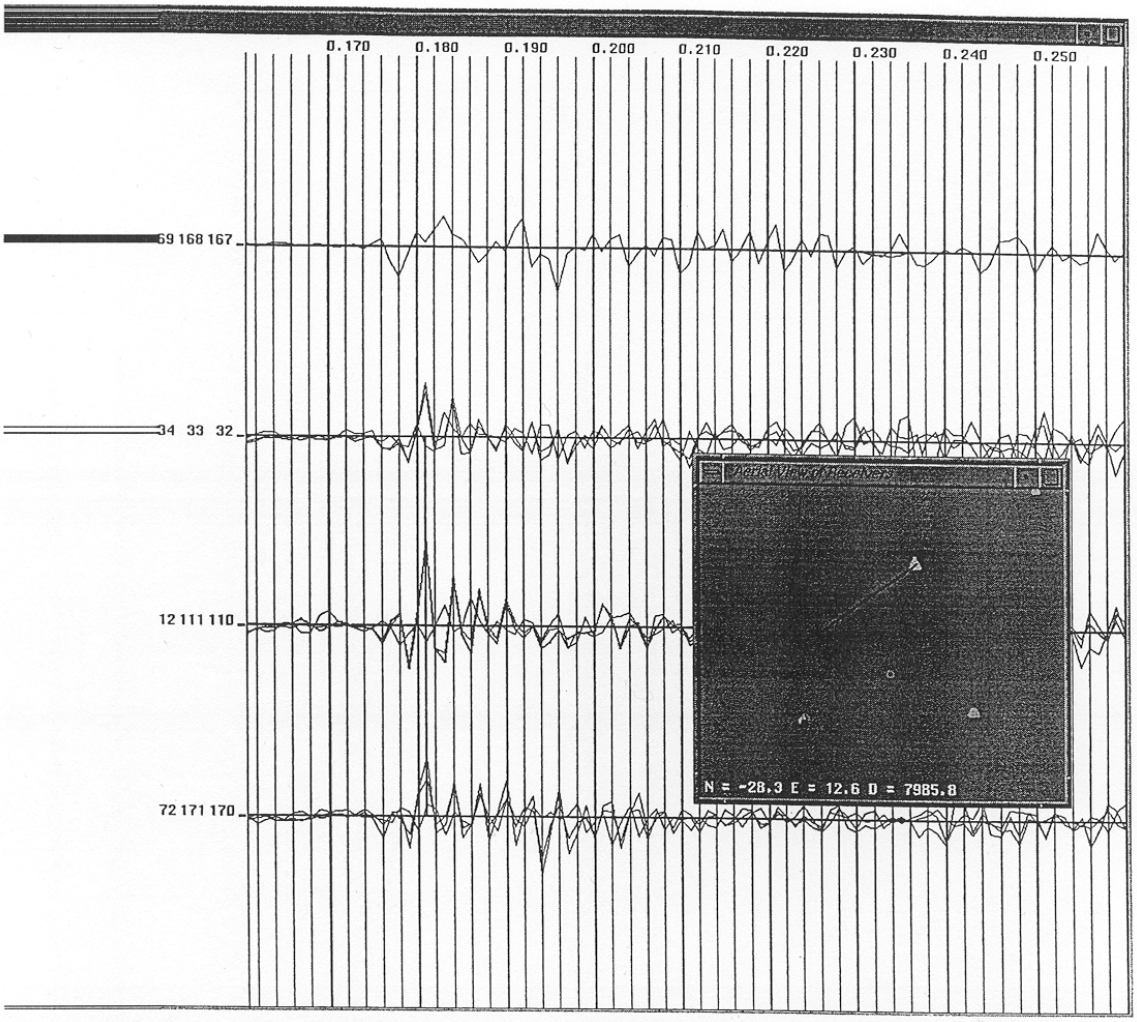

Primacord Hodogram Analysis - Pod 14

Figure 7

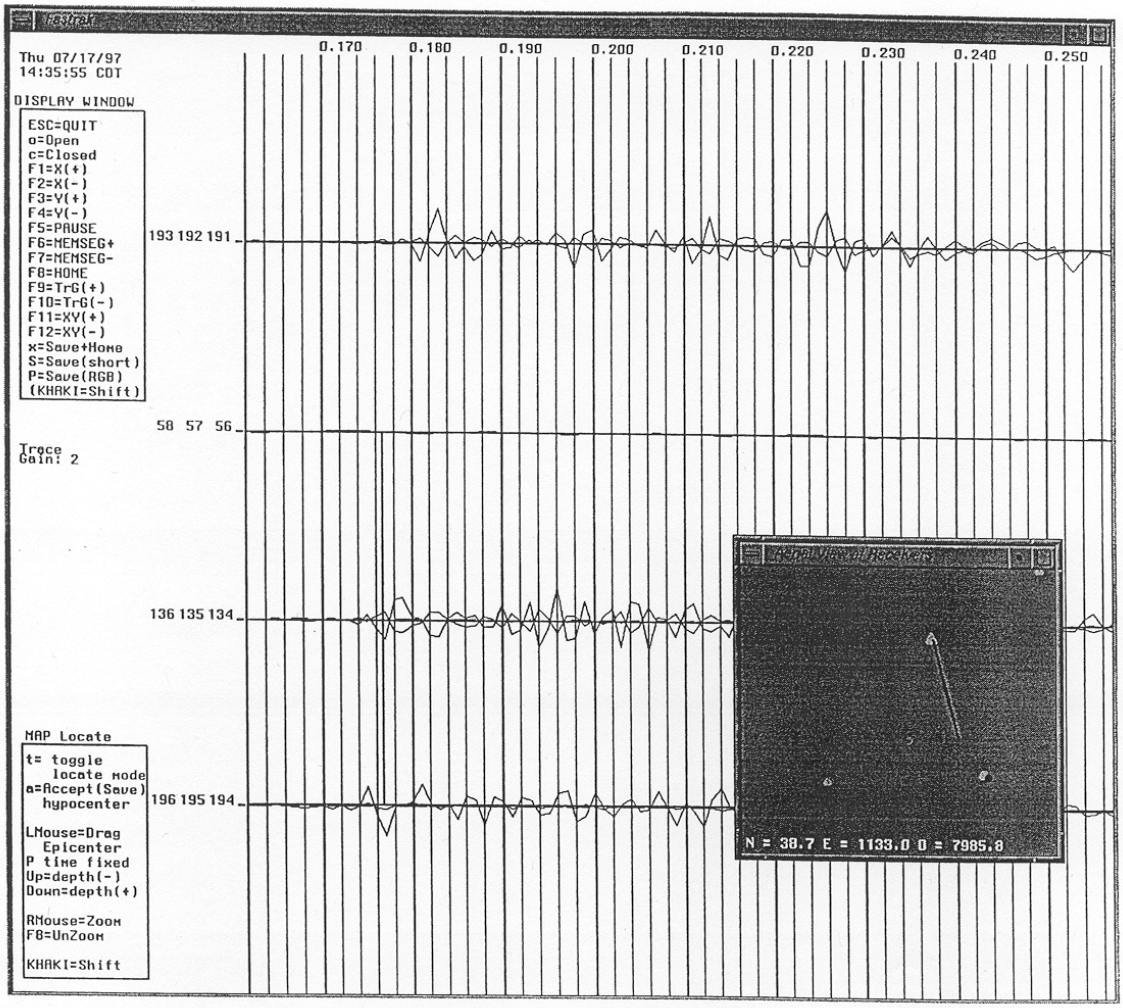

Perf Shot Hodogram Analysis - Pod 14

Figure 8

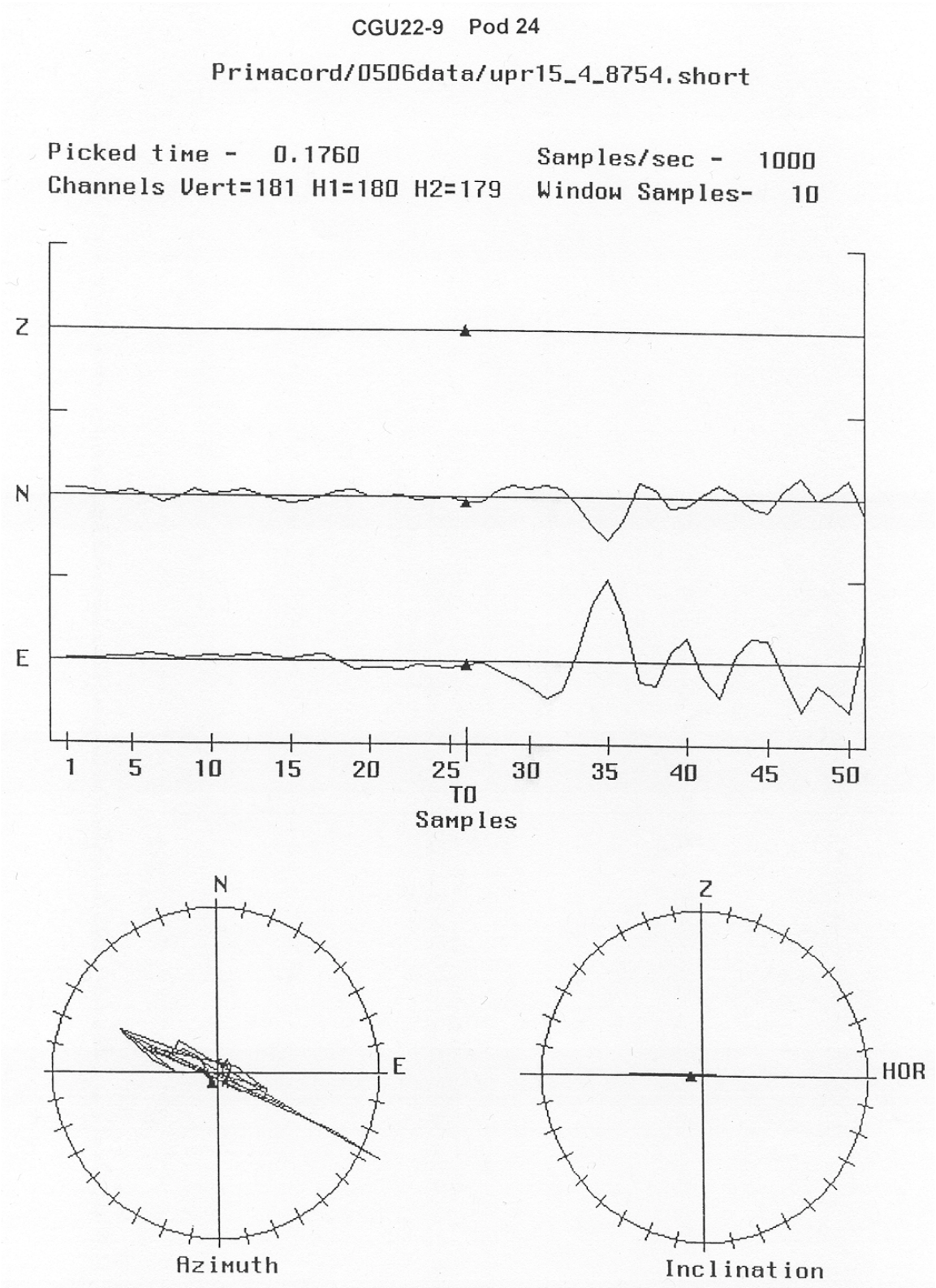
CGU22-9 Pod 24
Primacord/0506data/upr15_4_8754.short
Picked time - 0.1760
Samples/sec - 1000
Channels Vert=181 H1=180 H2=179
Window Samples- 10
Z
N
E
1
5
10
15
20
25
30
35
40
45
50
TO
Samples
N
E
Azimuth
Z
HOR
Inclination

Figure 9

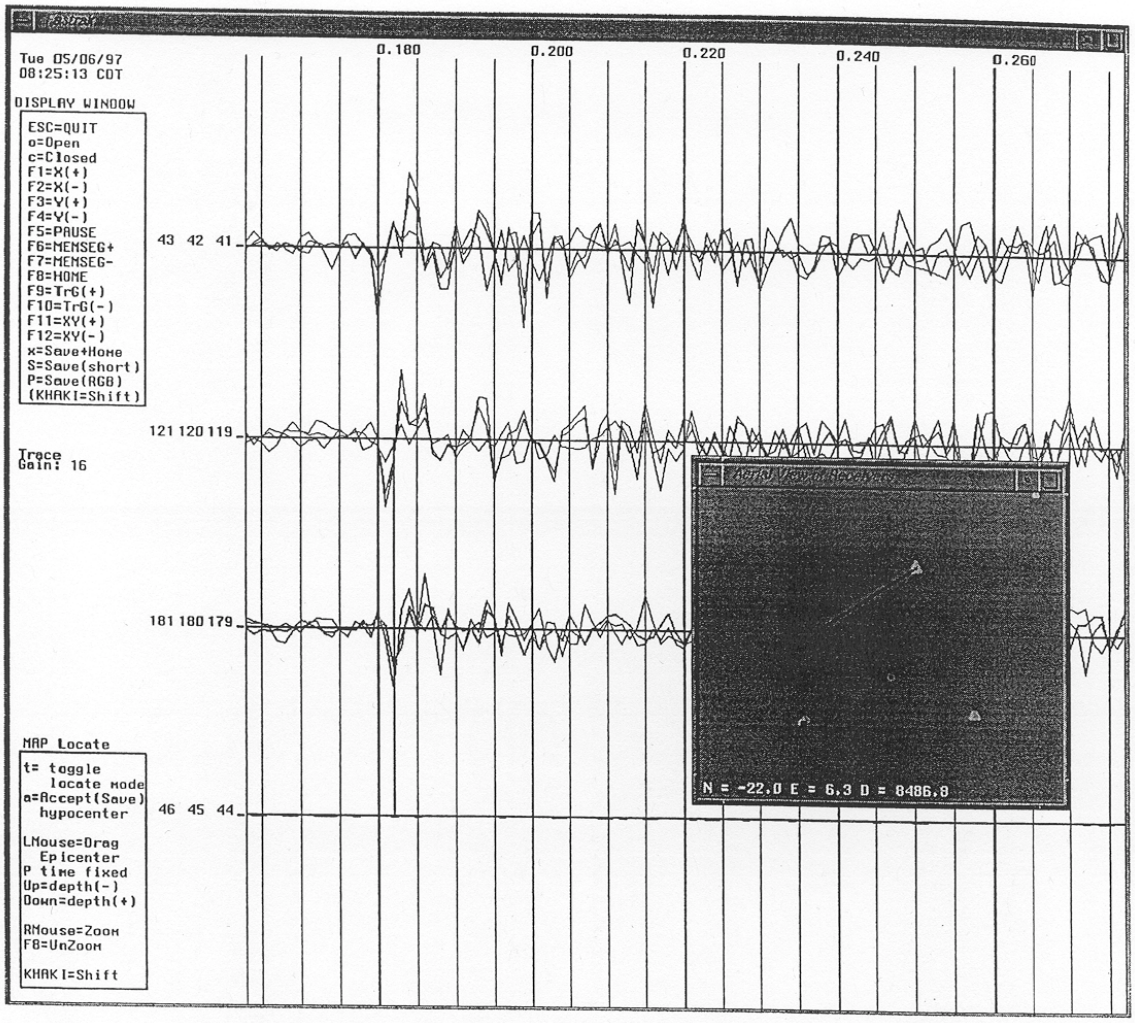

Primacord Hodogram Analysis - Pod 24

Figure 10

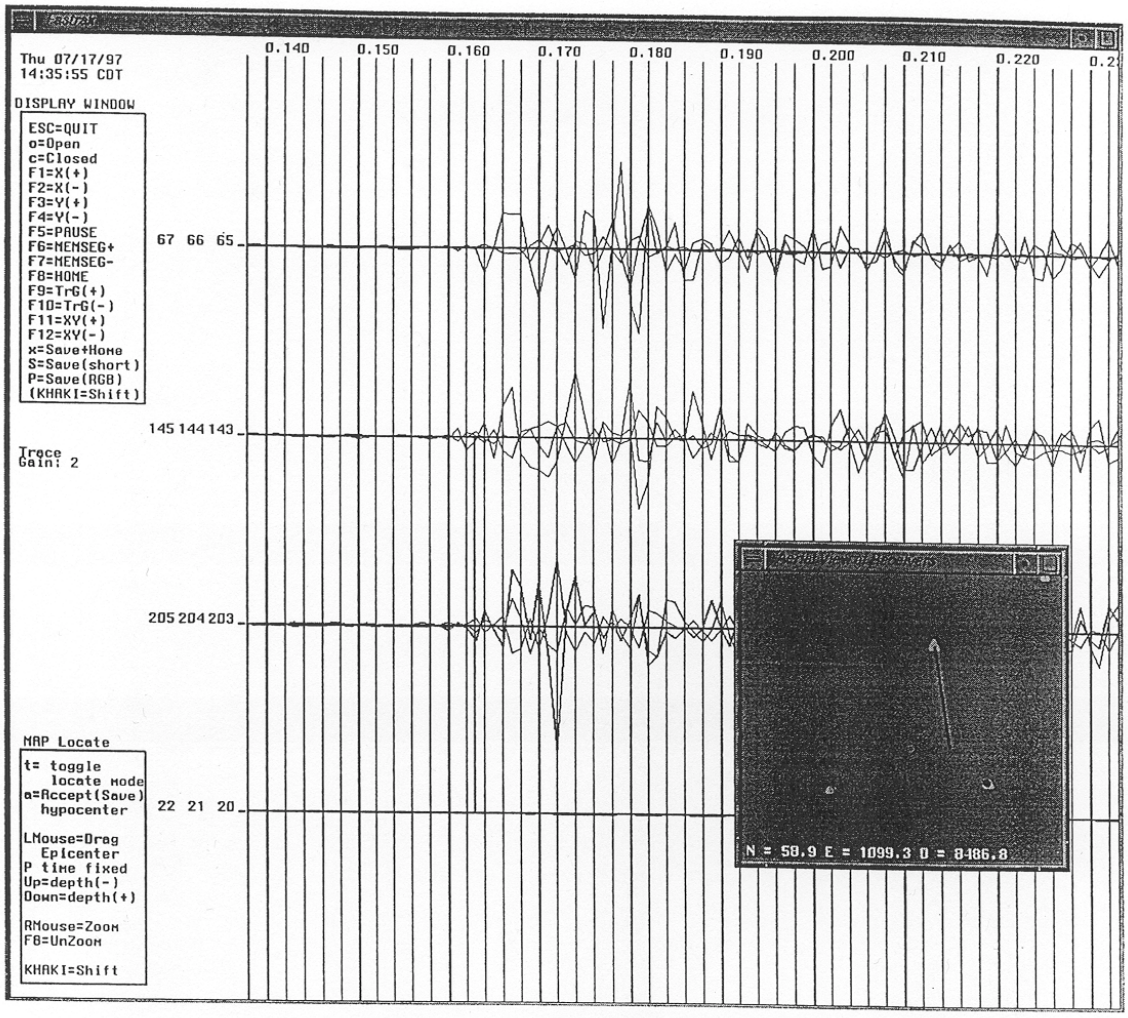

Perf Shot Hodogram Analysis - Pod 24

Figure 11

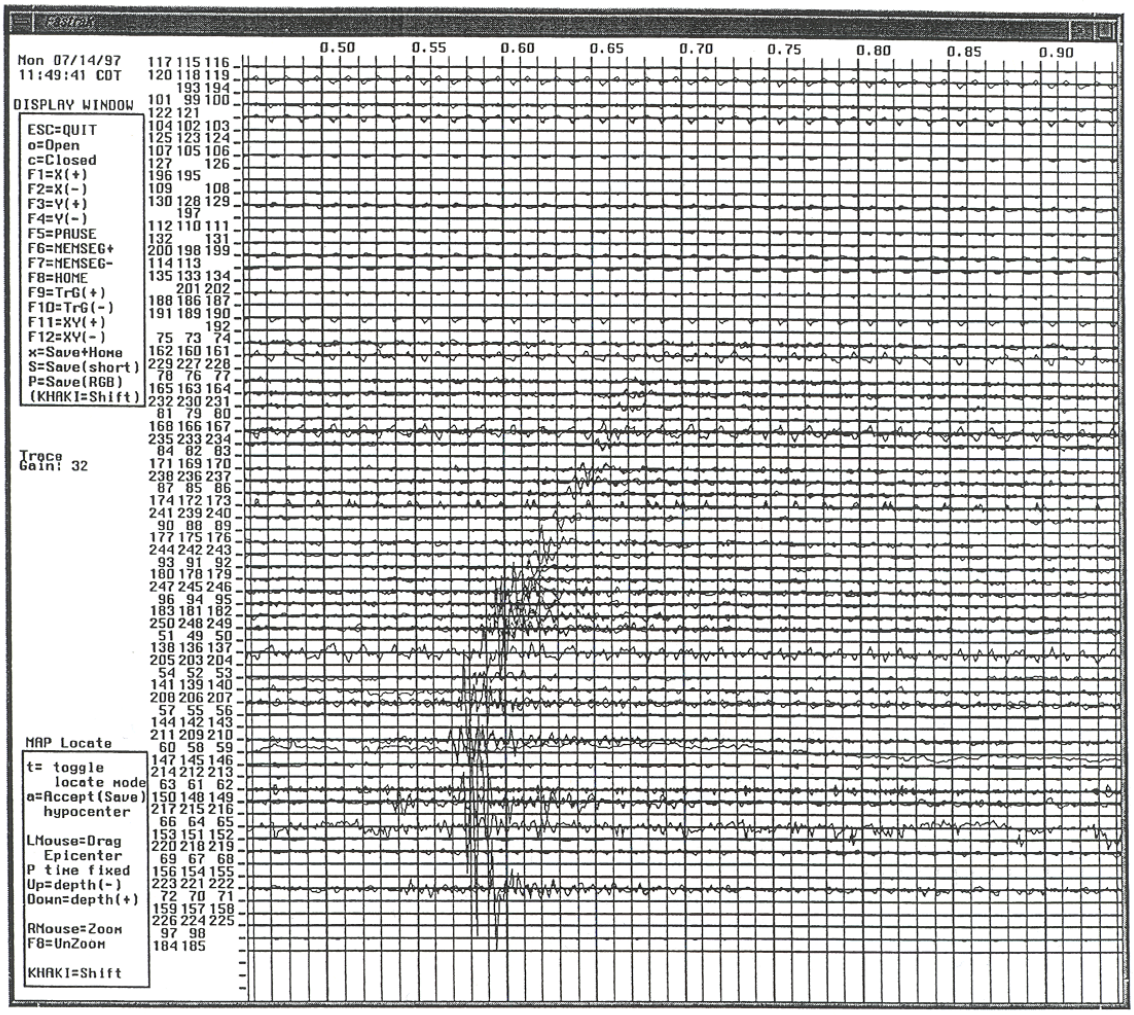

Typical Event - Shear Wave Energy Only

Figure 12

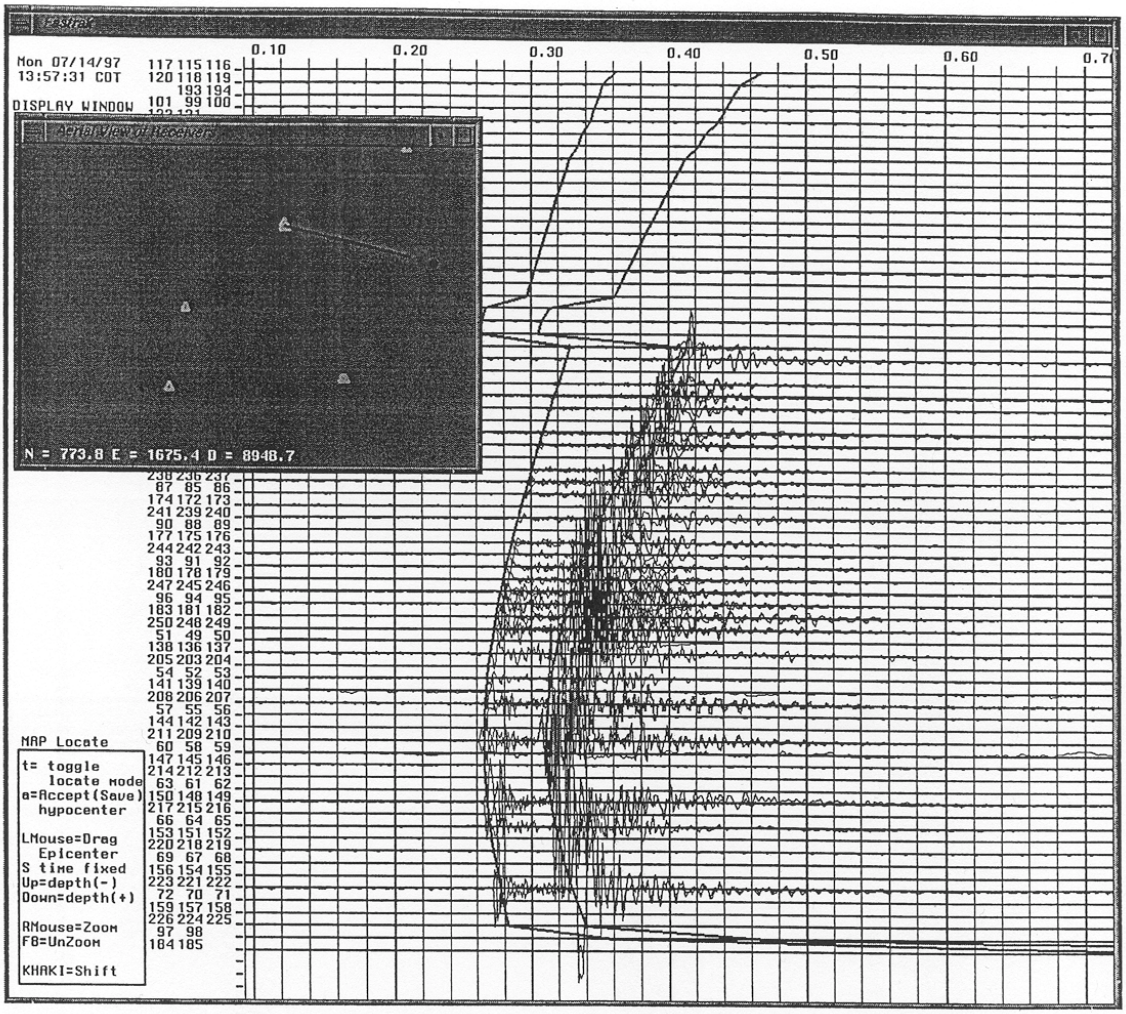

Good High Quality Event

Figure 13

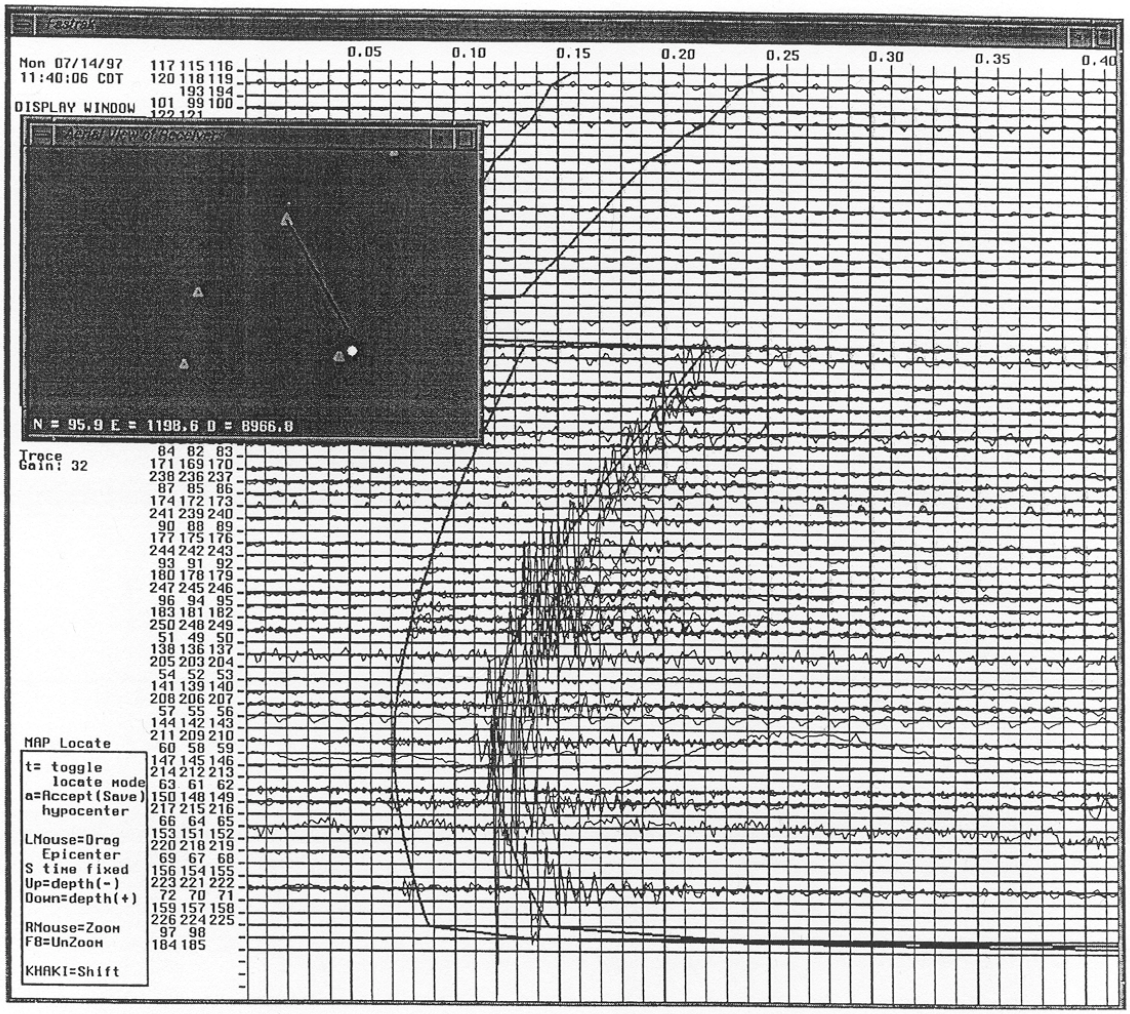

Typical Quality Event - Some Useable P Wave Energy

Figure 14

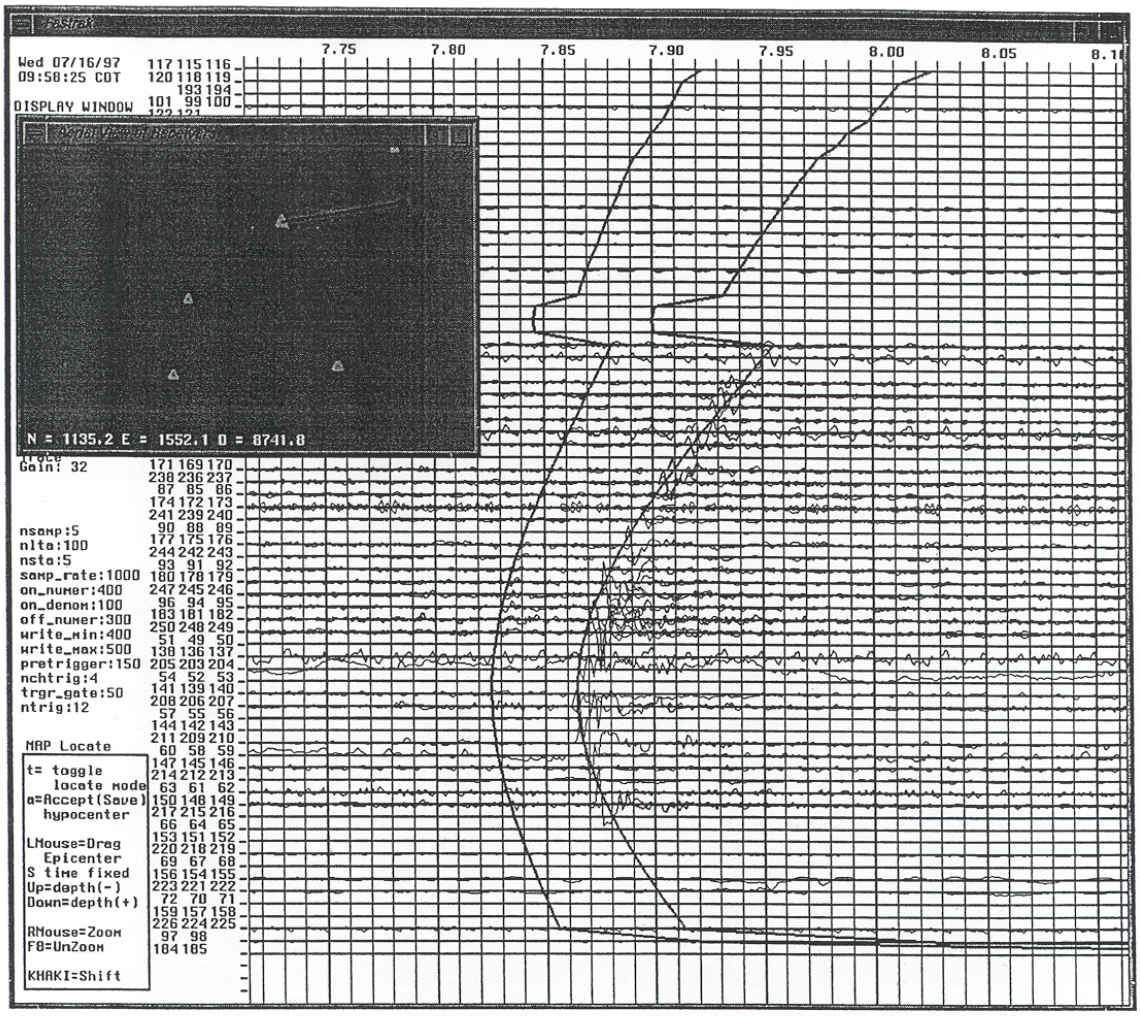

Typical Event Quality For 07/16/97

Figure 15

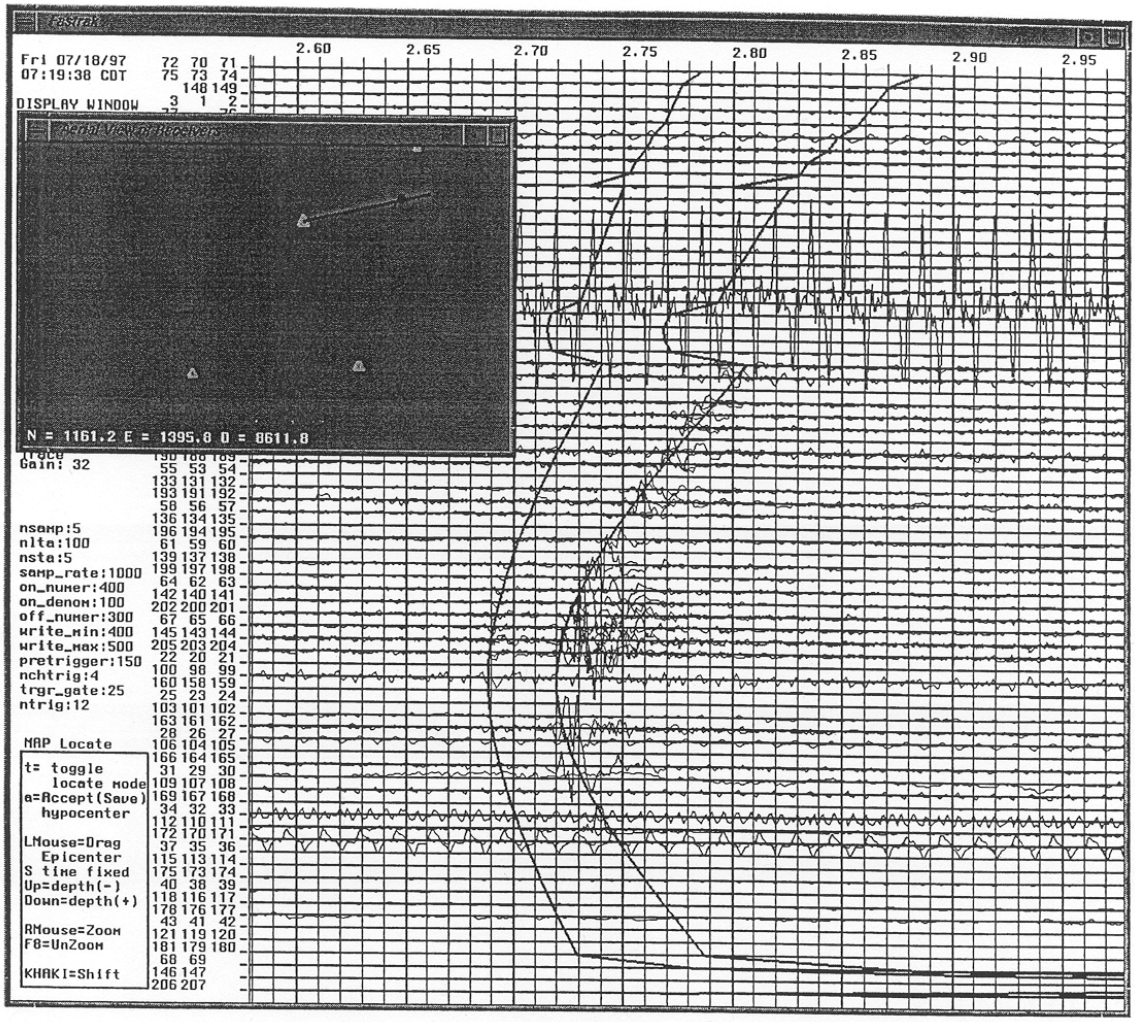

Typical Event Quality For 07/18/97

Figure 16

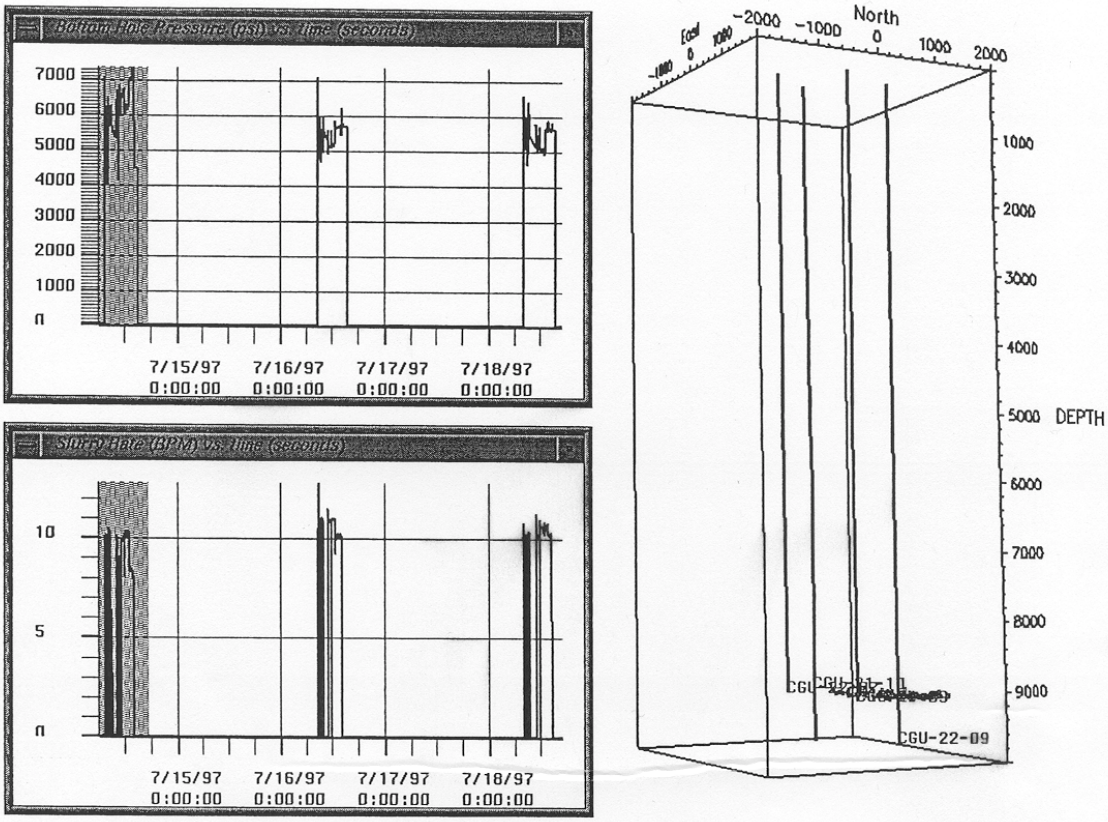

Event Locations For 07/14/97 (side view)

Figure 17

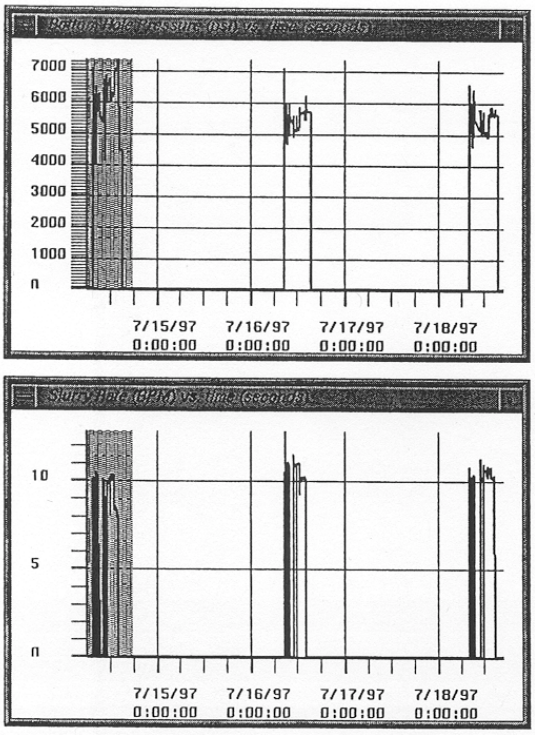

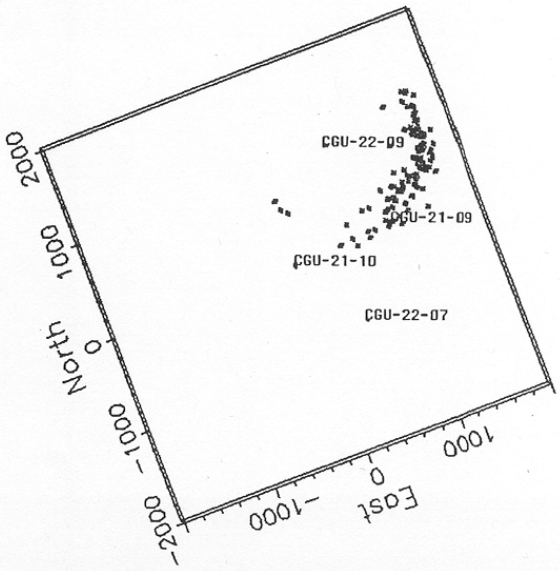

Event Locations For 07/14/97 (plan view)

Figure 18

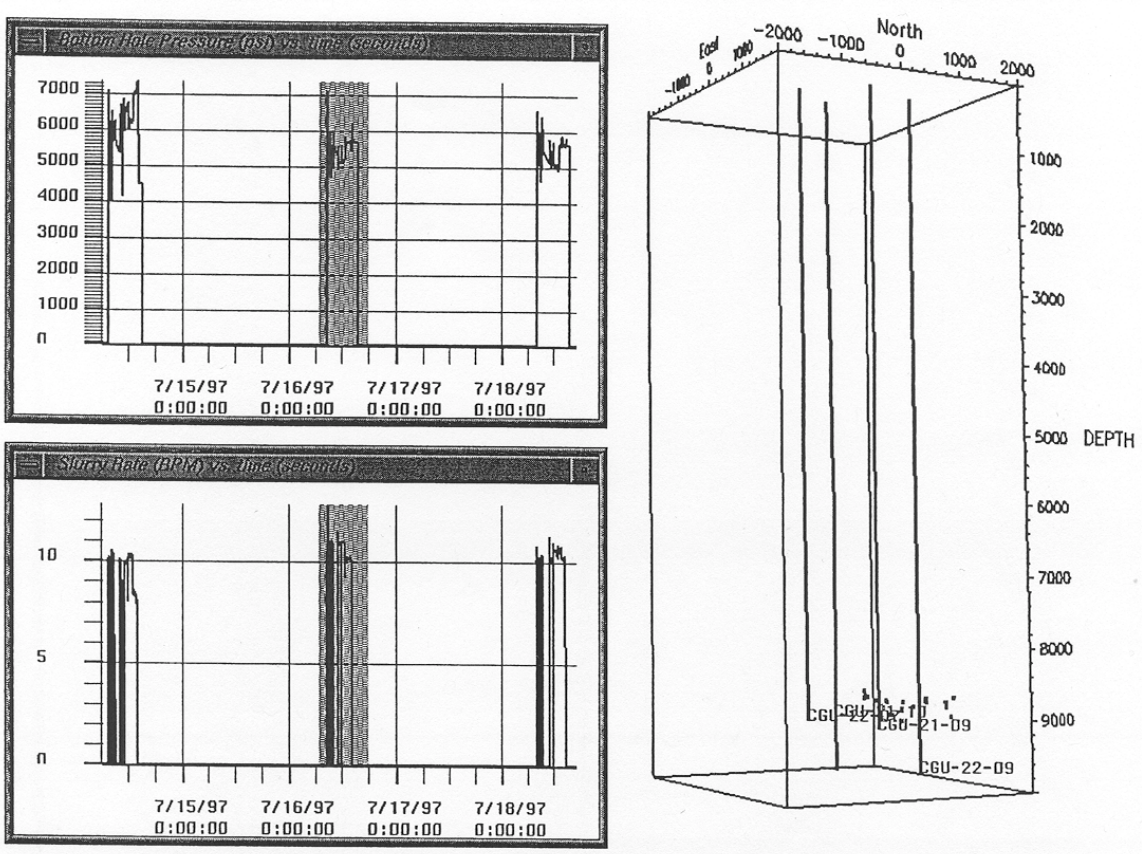

Event Locations For 07/16/97 (side view)

Figure 19

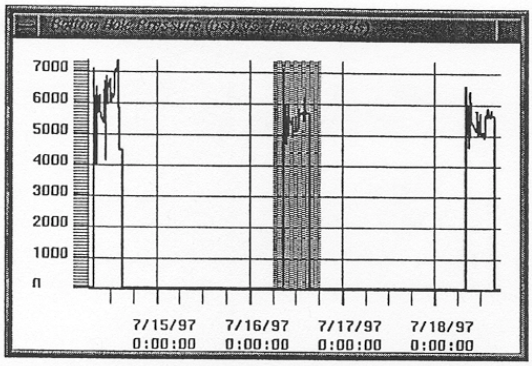

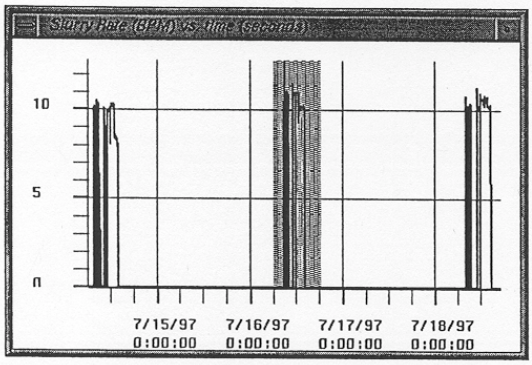

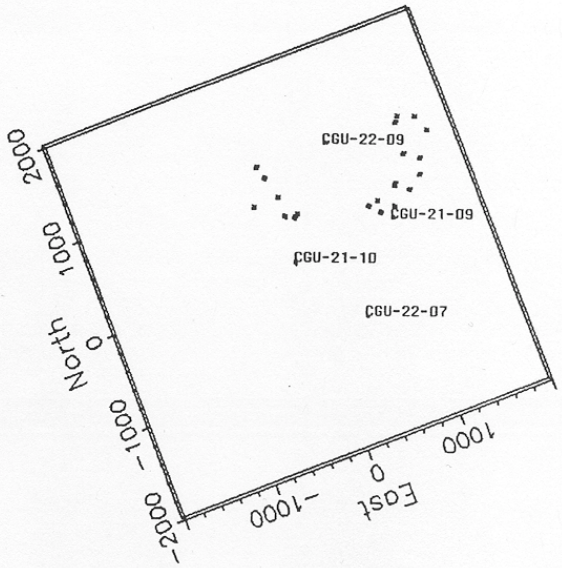

Event Locations For 07/16/97 (plan view)

Figure 20

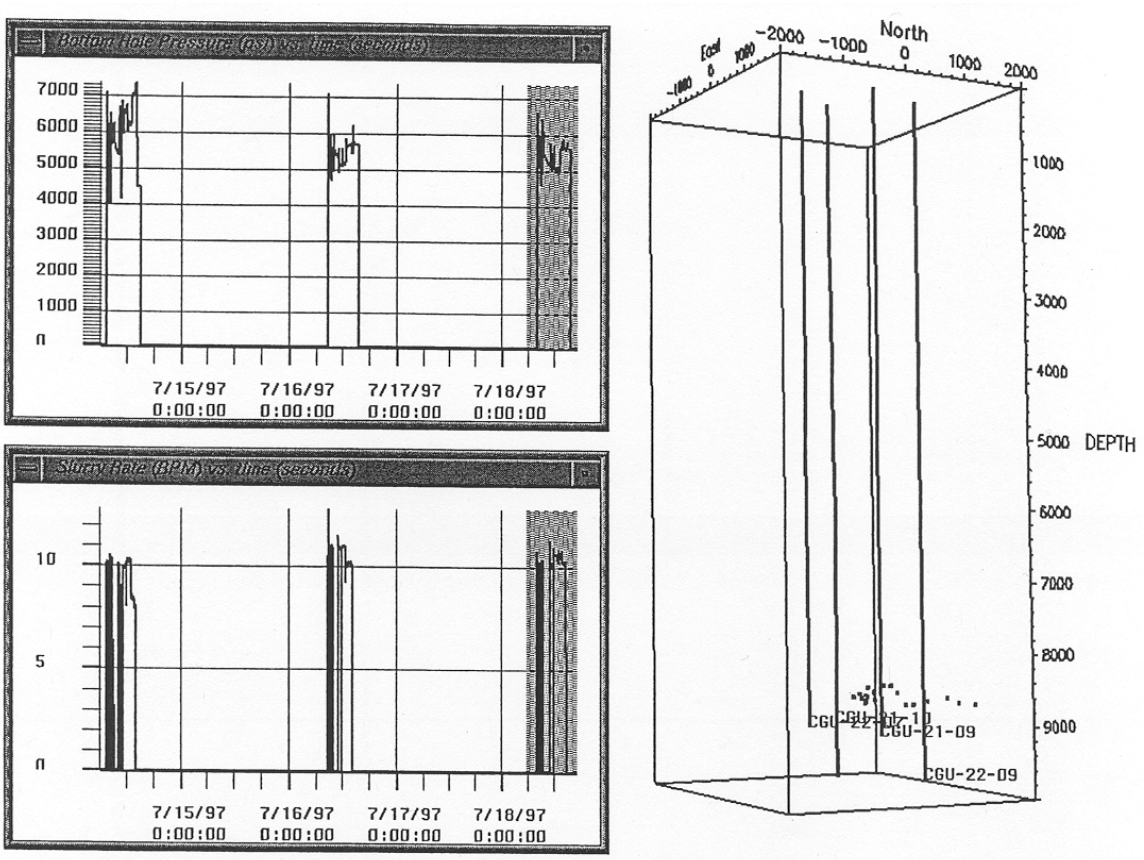

Event Locations For 07/18/97 (side view)

Figure 21

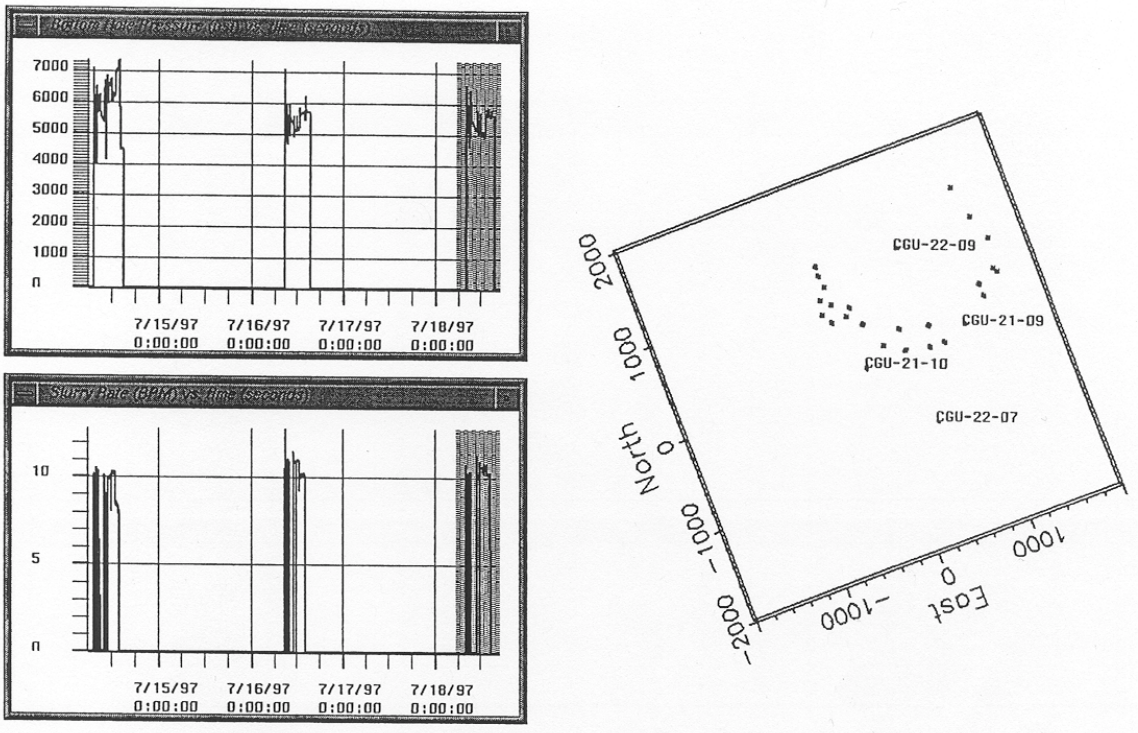

Event Locations For 07/18/97 (plan view)

Figure 22